Energy transfer between lasers in low-gas-fill-density hohlraums

A. L. Kritcher, J. Ralph, D. E. Hinkel, T. Döppner, M. Millot, D. Mariscal, R. Benedetti, D. J. Strozzi, T. Chapman, C. Goyon, B. MacGowan, P. Michel, D. A. Callahan, and O. A. Hurricane

Phys. Rev. E **98**, 053206 — Published 19 November 2018

DOI: 10.1103/PhysRevE.98.053206

Energy transfer between lasers in low gas-fill density hohlraums

A. L. Kritcher[1], J. Ralph[1], D. E. Hinkel[1], T. Döppner[1], M. Millot [1], D. Mariscal[1], R. Benedetti[1], D. J. Strozzi[1], T. Chapman[1], C. Goyon[1], B. MacGowan [1], P. Michel [1], D. A. Callahan[1], and O. A. Hurricane[1]
[1]*Lawrence Livermore National Laboratory, P.O. Box 808, Livermore, California 94551-0808, USA*
(Dated: October 1, 2018)

We investigate cross beam energy transfer (CBET), where power is transferred from one laser beam to another via a shared ion acoustic wave, for the first time in hohlraums with low gas fill density as a tool for late-time symmetry control for long pulse (>10ns) Inertial Confinement Fusion (ICF) and laboratory astrophysics experiments. We show that the radiation drive symmetry can be controlled and accurately predicted during the foot of the pulse (until the rise to peak power), which is important for mitigating areal density variations in the compressed fuel in ICF implosions. We also show that the effective inner beam drive after CBET is much greater than observed in previous high gas-filled hohlraum experiments, which is thought to be a result of less inverse bremsstrahlung absorption of the incident laser light and reduced ($>10x$) Stimulated Raman Scattering (SRS) (and Langmuir wave heating). With the inferred level of inner beam drive after transfer we estimate that $>1.25x$ larger plastic capsules could be fielded in this platform with sufficient laser beam propagation to the waist of the hohlraum. We also estimate that a full scale plastic capsule, 1100 μm in capsule radius, would require ∼1-2 Angstroms of 1ω wavelength separation between the outer and inner beams to achieve a symmetric implosion in this platform.

Laser driven multi-millimeter x-ray radiation environments lasting longer than ten nanoseconds are relevant for Inertial Confinement Fusion (ICF) experiments [1, 2] and laboratory astrophysics experiments [3, 4]. These long-duration radiation drives are achievable at the National Ignition Facility (NIF) [5] using laser irradiated gold or uranium hohlraums. However, time-dependent asymmetries in these radiation environments are difficult to diagnose and control due to plasma filling of the hohlraum and impaired late-time laser beam propagation [6–10]. Experiments using ramped laser pulses lasting tens of nanoseconds to study material properties require symmetry for accurate interpretation of radiography or velocimetry data. In addition, radiation drive asymmetries are important for ICF experiments and are thought to have been one of the limiting factors in the performance of the successful HiFoot campaign [2, 11–13], which mitigated instabilities at the ablation front with a higher picket radiation temperature than preceding experiments. Simulations suggest that if these hohlraum drive asymmetries were mitigated the neutron yield could be further increased [14, 15].

Such experiments transferred power between crossing laser beams (Cross Beam Energy Transer (CBET)) [16] operating at different wavelengths via Stimulated Brillouin Scattering (SBS) [17], a three-wave process between two crossing beams and an ion acoustic wave generated by their beat wave. This process has been utilized to modify radiation drive symmetry during the peak of the pulse in high gas-filled hohlraums (0.96 - 1.6 mg/cc He) [11, 18–21]. However, symmetry during the early part of the drive was difficult to predict and control due to laser-plasma interactions. Controlling these early-time asymmetries is important because they can cause significant variations in the areal density of the compressed shell and can limit compression and heating of the Deuterium-Tritium (DT) fuel in ICF experiments. In addition, swings in the radiation flux symmetry as a function of time can result in swings between the in-flight and hot-spot symmetry, resulting in an overestimation of the amount of CBET needed to drive a round implosion.

Following these experiments, there has been a significant effort to control time-dependent radiation drive asymmetries without the use of CBET, which has been achieved through shorter duration experiments using alternate higher density HDC (High Density Carbon) and Beryllium ablators [22–25] and smaller capsules [26]. These experiments have increased the size of the hohlraum compared to the capsule size to improve inner beam propagation and moved to lower hohlraum gas fill densities (0.3-0.6 mg/cc He) to increase laser energy coupling to the hohlraum [27, 28]. The early radiation drive asymmetries, before the peak of the radiation drive, were significantly improved compared to previous experiments [26]. However, late-time laser beam propagation to the waist of the hohlraum remains a concern for fielding larger capsules and for experiments using plastic ablators that require longer pulses. For example, implosions using plastic ablators at full scale (1100μm) with no intentional CBET resulted in elongation of the dense shell in flight and final hot spot shape along the equatorial plane (oblate implosion) which is expected to significantly impact the neutron yield (by >70% according to simulations [7]).

Here, we demonstrate for the first time the effectiveness of using CBET in hohlraums with low gas fill density (0.6 mg/cc He) that have demonstrated high laser coupling [26, 28], to increase late time inner beam propagation. We also show that we can accurately predict and control early time drive asymmetries compared to those

seen in high gas-filled hohlraums. In these experiments, energy was transferred from the outer beams to the inner beams using a 1ω wavelength separation ($\Delta\Lambda$) of 2-5.5 Angstroms ($\mathring{A}$) between the outer and inner beams. This transfer results in enhanced late-time drive at the waist of the hohlraum with the intent to drive the implosion more prolate, or elongated along the axis of the hohlraum. Measured shock velocities along the pole and equator [29, 30] during the foot of the laser pulse (until the rise to peak power) were predictable and agree well with simulations. Measured inflight implosion symmetry [31] suggests a significant increase in effective inner beam drive after CBET compared to previous experiments and compared to pre-shot predictions. Given this enhanced level of late-time drive at the waist of the hohlraum, we provide an estimate for the largest capsule we could drive round in this platform and the level of $\Delta\Lambda$ required to achieve a round implosion.

The experiments were performed at NIF using plastic GDP (glow discharge polymer) ablators with a graded Si dopant layer to shield against preheat from hohlraum x-rays. The outer diameters of the capsules were 1110μm and the ablator thicknesses were 175-188 μm. The capsules were filled with liquid D2 for the shock tuning experiments, N161103-001 and N161006-002, and a gas mixture of D^3He for the experiment to measure inflight symmetry using x-ray radiography, N170706-001, see Fig.1 (bottom right). Shot N161006 used a wavelength separation of $\Delta\Lambda = 2\mathring{A}$ between the inner and outer beams and N161103 and N170706 operated at $\Delta\Lambda = 5.5\mathring{A}$. Shot N170706 also separated the inner cone wavelengths, or three-color $\Delta\Lambda$ see Table 1 of the appendix. The hohlraum was 6.72 mm in diameter, 11.24 mm in length, and had a 3.64 mm diameter laser entrance hole (LEH). The hohlraum wall material was Depleted Uranium (DU) for N161103 and gold-lined DU for N170706. A schematic of the hohlraum configuration with example simulations overlaid is shown in Fig.1. See also J. Ralph, *et al.* [32] for more details regarding the experimental configuration and results.

Laser powers vs time for the tuning shots operating at $\Delta\Lambda = 5.5\mathring{A}$ (N161103 and N170706) are shown in Fig.1. Differences in the pulse shapes were made to separate the shock mergers for N161103 [30], account for the change in hohlraum wall material, and improve ablation front stabilization via a stronger first shock for N170706. The total energy of shot N161103 was limited compared to N170706 due to the risk of laser light backscatter into the optics. Both pulses delayed the outer beams by 1.2 ns compared to the inner beams to provide time for the inner beams to blow down the window covering the LEH. The cone fractions during the foot of the pulse (until the rise to peak power at $\sim$ 11 ns) were designed to mitigate early time asymmetries induced by the cross-beam energy transfer that occurs over the duration of the entire pulse, see Fig.1 (inset).

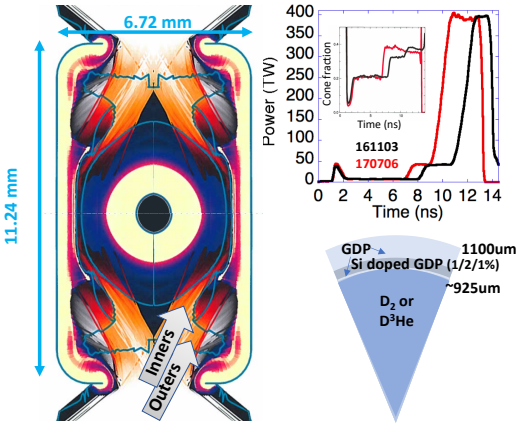

FIG. 1. Schematic of the hohlraum (left hand side) with simulations overlaid showing the trajectory of the inner and outer beams. A diagram of the GDP capsule configuration is shown in the bottom right, including the silicon doped layers. The laser powers vs time are shown in the upper right hand side for the shock timing (N161103, in black) and radiography (N170706, in red) shots. Also included are the measured cone fractions as an inset.

The hohlraum radiation drive and capsule were modeled together using the radiation hydrodynamics code HYDRA [33] in two dimensions with an axis of symmetry along the hohlraum axis. The radiation drive was calculated using the so-called "high-flux model" [34] with detailed configuration accounting (DCA) non-local thermodynamic equilibrium (NLTE) atomic physics and Spitzer-Härm electron thermal conduction with a flux-limiter of $0.15 n_e T_e v_{Te}$. Here, n_e is the electron density, T_e is the electron temperature, and v_{Te} is the electron thermal velocity. The emissivities and opacities were calculated inline using DCA for T_e >300 eV and using local thermodynamic equilibrium (LTE) tables elsewhere. Tabular equations of state, LEOS (Livermore Equation Of State), and tabular opacities (OPAL) [35] were used to model the GDP ablator.

The as-shot laser energies and backscatter [36] were measured and used as inputs to the simulations. Multipliers on the laser power during the foot of the pulse [37] were determined from separate calibration experiments with no intentional CBET [38]. In addition, a laser power multiplier applied during the peak of the drive was needed to match the time of maximum hotspot x-ray emission [39] for shot N170706 (14.7 ± 0.04) while correcting for the loss of drive due to the hohlraum diagnostic windows not present in the simulations. The time-dependent CBET was calculated from simulations with the full laser power and included in subsequent simulations where the incident laser power was modified to account for backscatter and to reproduce measured shock velocities [16]. This method has been shown to overestimate inner beam drive in experiments at high

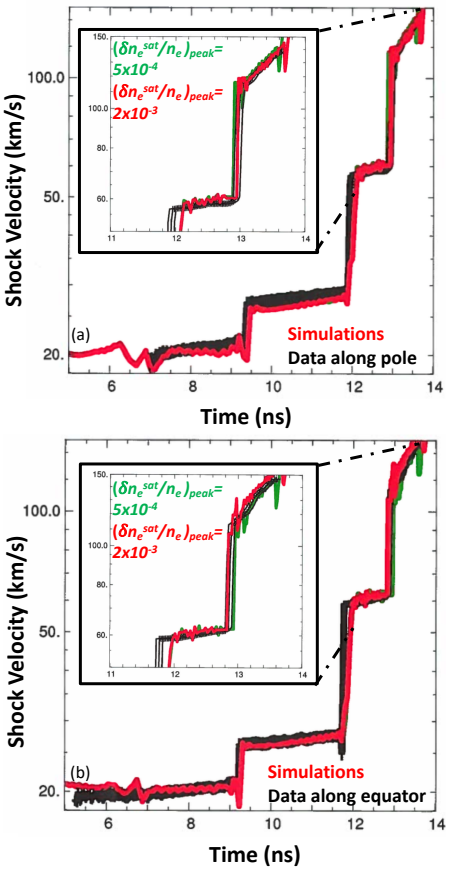

FIG. 2. (a) Simulated shock velocities (km/s) vs time in the polar direction (red and green) compared to experimental data (black) for shock timing shot N161103. (b) Simulated (red and green) vs measured (black) shock velocities along the equatorial direction for N161103. The insets are expanded views of the final shock mergers to show model sensitivity. The three experimental curves correspond to the uncertainty range of the measurement.

hohlraum gas fill density, and where there is significant laser backscatter on the inner beams (Stimulated Raman Scattering (SRS), i.e., the process whereby incident laser light resonantly scatters off Langmuir waves)[40]. Impact of laser beam absorption via inverse bremsstrahlung, energy into Langmuir waves, or reabsorption of backscattered light, are not included which reduce the amount of inferred transfer, but better approximate low-gas-fill hohlraum experiments (as described here), with $>10x$ lower SRS.

During the foot of the pulse we do not use artificial multipliers on the symmetry. However, during the peak of the drive we apply an empirically determined saturation clamp ($\delta n_e^{\rm sat}/n_e$) on the level of electron density fluctuation associated with the ion acoustic wave, effectively reducing CBET. Such an artificial clamp is routinely used in radiation hydrodynamic modeling to match experimental observables, e.g. [41, 46], and is still required (albeit at a larger value) when SRS and CBET are self consistently modeled inline [40]. In the foot of the drive we use $\delta n_e^{\rm sat}/n_e$=1x10^{-2} which is effectively unsaturated since the plasma waves driven by CBET typically range from $\delta n_e/n_e$ = 1x10^{-4} – 1x10^{-3} [47].

Measured shock velocities as a function of time are shown in Fig. 2 for shot N161103 (black curves where the error is denoted by the width), with distinct features corresponding to the first shock breaking out of the ablator into the D2 (∼9.3ns), merger of the first and second shocks (∼11.9ns), and merger of the first and second shocks with the final shock (∼12.9ns). Measurement of shock velocities along the polar direction (Fig. 2 (a)) and equatorial direction (Fig. 2 (b)) provide information on the symmetry of the shocks as a function of time. Loss of data occurs at velocities exceeding ∼140 km/s due to pre-heating from self emission of the shock front. The data are well matched by simulations (red curves) during the foot of the pulse (until the final shock merger) using a nearly unsaturated level of cross beam energy transfer and without the need for artificial symmetry multipliers. This model also accurately reproduced measured shock velocities at lower levels of wavelength separation $\Delta\Lambda = 2\mathring{A}$ (shot N161006-002). In contrast, matching measured shock velocities in high-gas fill hohlraums, where modeling of beam propagation and plasma conditions was difficult, required artificial multipliers on the drive symmetry during the foot of the pulse.

However, a saturation clamp on CBET during the peak of the pulse was required to match the final shock mergers and velocities, see Fig. 2 insets for expanded views of the final mergers. Due to sensitivity of the diagnostic a range of $\delta n_e^{\rm sat}/n_e$ (5x10^{-4} (*green*) - 2x10^{-3} (*red*)) applied during the rise and peak of the pulse, corresponding to ∼1.36-1.6x average effective inner beam power increase, matched experimental data. Here, higher $\delta n_e^{\rm sat}/n_e$ corresponds to increased transfer from the outer to inner beams and a faster final shock along the equator. To narrow down this range, a more sensitive follow on tuning experiment was fielded where the dense shell symmetry at a convergence of ∼5 (inflight) and hot spot core emission symmetry were measured.

Figure 3 shows simulated radiographs of the dense shell inflight for shot N170706 at a radius of ∼200μm, along with simulated Legendre decompositions (l = 2 component) of the limb minimum transmission contour (red points) as a function of $\delta n_e^{\rm sat}/n_e$ applied during the peak of the pulse. The x-axis at the top of the plot is the amount of calculated increase in average inner beam power as a result of the cross-beam energy transfer. The measured radiograph at ∼200μm is also shown, along with a blue band corresponding to the l = 2 (P2) moment of the measured limb minimum transmission contour with error bars. A range of $\delta n_e^{\rm sat}/n_e$ = 2 – 3x10^{-3} reproduces the measured inflight symmetry which overlaps with the upper bound of the range used to match the final shock symmetry for N161103, when accounting

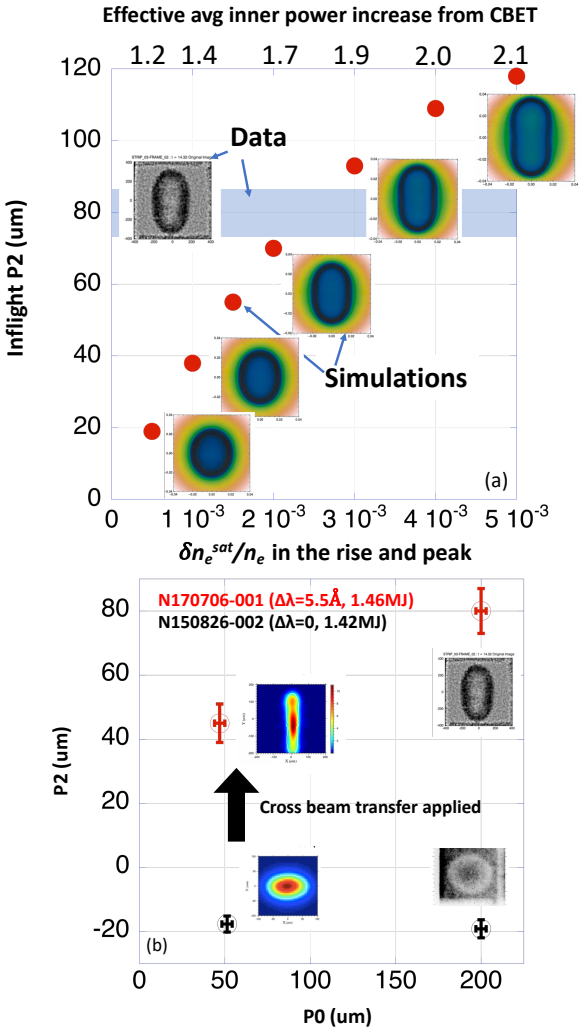

FIG. 3. (a) Simulated radiographs and P2 decompositions (red points) of the dense shell inflight (radius near 200μm) for shot N170706 vs effective average power increase on the inner beams as a result of CBET (top x-axis). The simulations saturate the amplitude of the ion acoustic wave ($\delta n_e^{\rm sat}/n_e$) to vary the x-axis (shown on the bottom x-axis). Also shown is the measured radiograph and P2 with a band that denotes the uncertainty. (b) Decompositions of the measured P2 inflight (P0=200μm) and near peak compression (P0$\sim$50μm) for low-gas-fill hohlraum experiments with no intentional CBET (N150826: $\Delta\Lambda$=0$\AA$) and with CBET (N170706: $\Delta\Lambda$=5.5$\AA$).

for the changes made between the shots including the $\Delta\Lambda$ change. The calculated level of average inner beam power increase during the rise and peak of the pulse for N170706 and $\delta n_e^{\rm sat}/n_e \sim 2-3{\rm x}10^{-3}$ is 1.67 - 1.9x, which is higher than calculated for HiFoot shot N140520 (1.26x) operating at a hohlraum gas fill density of 1.6 mg/cc He and similar wavelength separation, $\Delta\Lambda = 6.2\AA$.

In addition, the effective inner beam power was significantly increased compared to a benchmark experiment in a low-gas-fill hohlraum with no intentional CBET [26] (N150826: $\Delta\Lambda$=0$\AA$) which resulted in an oblate inflight dense shell and hot spot, see Fig. 3 (b). The change in $l = 2$ moment (P2) between the inflight and hot spot symmetry [45] (non-conformal P2) for N170706 is thought to be due to cooling of the outer regions of the hot spot. This experiment used the same target configuration and pointing, same hohlraum gas fill density (0.6 mg/cc), similar laser energy (N150826$\sim$1.42MJ vs N170706$\sim$1.46 MJ), similar pulse length (N150826$\sim$13.6ns vs N170706$\sim$13.2ns), and similar laser cone fraction during the peak of the pulse (N150826$\sim$34% vs N170706$\sim$35%). The main difference between these experiments was adjustment to the foot of the pulse to achieve symmetry for $\Delta\Lambda$=0$\AA$ vs 5.5$\AA$. Other diagnostics that support increased effective inner beam drive after CBET include a significant increase in the measured inner beam SBS [32, 42, 43] compared to experiments with no intentional transfer and increased hard x-ray self emission from interaction between the inner beams and the hohlraum wall near the equator [32, 44].

The improved waist drive after in transfer in low-gas-fill hohlraums over that of high gas-fill hohlraums is in part due to less inverse bremsstrahlung absorption of laser light along the beam path and reduced (>10x) SRS backscattered laser energy [32] (and Langmuir wave heating). Fewer super-thermal electrons were also observed in these experiments compared to high-gas fill [22, 32, 48], which is consistent with the reduced SRS. Previous analysis of high-gas-fill hohlraum experiments [40] speculated improved transfer for platforms with reduced SRS, which is demonstrated for the first time in this work. More self-consistent modeling of electron transport, CBET, and backscatter, though less important for the low-gas-filled hohlraums, should further mitigate the need for an empirically determined saturation level in simulations [40].

An excess of drive on the waist of the hohlraum can be used advantageously to drive larger capsules which reduces the energy requirement for ignition due to higher convergence. Using $\delta n_e^{\rm sat}/n_e = 2-2.5{\rm x}10^{-3}$ we estimate that transfer to the inner beams, resulting in 1.7-1.9x increase in average laser power, could enable driving >25% larger capsules (>1400μm in outer radius), with the same thickness, which could result in more than 2.5 times yield improvement from analytical scaling of yield with capsule size [49] and more if alpha heating is considered. For this design study $\Delta\Lambda = 5\AA$ between the inner and outer beams was used, consistent with N161103, which gave reduced laser backscatter compared to N170706 [42]. In addition, we estimate that a nominal full scale capsule (1100μm) with a 1.8 MJ laser pulse could be driven symmetrically with a wavelength separation of $\Delta\Lambda = 1-2\AA$. The calculated hot spot P2 using $\delta n_e^{\rm sat}/n_e = 2-2.5{\rm x}10^{-3}$ is -3 to $+4.5\mu$m for $\Delta\Lambda = 1\AA$, and 19-22μm prolate for $\Delta\Lambda = 2\AA$.

In summary, we have investigated cross-beam energy

transfer from the outer to inner beams for the first time in low-gas-fill hohlraums with the intent to increase the radiation drive at the waist of the hohlraum and drive the implosion more prolate. We found that the amount of effective increase in inner beam drive at a given wavelength separation was higher than predicted and higher than observed in high-gas filled experiments. We showed that the foot of the drive can be accurately predicted and controlled in low-gas-fill hohlraums in the presence of CBET without artificial multipliers on the radiation drive symmetry. With this magnitude of drive at the hohlraum waist we estimate that large plastic capsules exceeding 1400 μm in outer radius could be driven symmetrically for a 1.8 MJ laser pulse. We also predict that an outer to inner beam wavelength separation of 1-2$\AA$ would result in a round implosion for a nominal capsule outer radius of 1100μm and a 1.8 MJ pulse. Following this work, the ICF program has launched a new campaign to use CBET in low-gas-fill hohlraums to enable driving time-dependent symmetric implosions with 1100μm plastic ablators and is also being considered by the ICF program to field larger diamond ablator implosions than have ever been shot before on the NIF.

ACKNOWLEDGEMENTS

This work performed under the auspices of the U.S. Department of Energy by Lawrence Livermore National Laboratory under Contract No. DE-AC52-07NA27344. This document was prepared as an account of work sponsored by an agency of the United States government. Neither the United States government nor Lawrence Livermore National Security, LLC, nor any of their employees makes any warranty, expressed or implied, or assumes any legal liability or responsibility for the accuracy, completeness, or usefulness of any information, apparatus, product, or process disclosed, or represents that its use would not infringe privately owned rights. Reference herein to any specific commercial product, process, or service by trade name, trademark, manufacturer, or otherwise does not necessarily constitute or imply its endorsement, recommendation, or favoring by the United States government or Lawrence Livermore National Security, LLC. The views and opinions of authors expressed herein do not necessarily state or reflect those of the United States government or Lawrence Livermore National Security, LLC, and shall not be used for advertising or product endorsement purposes.

[1] M. J. Edwards, P. K. Patel, J. D. Lindl, L. J. Atherton, S. H. Glenzer, S. W. Haan, J. D. Kilkenny, O. L. Landen, E. I. Moses, A. Nikroo, *et al.*, Phys. Plasmas **20**, 070501 (2013).

[2] O. A. Hurricane, D. A. Callahan, D. T. Casey, P. M. Celliers, C. Cerjan, E. L. Dewald, T. R. Dittrich, T. Doeppner, D. E. Hinkel, L. F. Berzak Hopkins, *et al.*, Nature, **506**, 343 (2014).

[3] R. F. Smith, J. H. Eggert, R. Jeanloz, T. S. Duffy, D. G. Braun, J. R. Patterson, R. E. Rudd, J. Biener, A. E. Lazicki, A. V. Hamza, J. Wang, T. Braun, L. X. Benedict, P. M. Celliers, and G. W. Collins, Nature **511**, 330 (2014).

[4] D. E. Fratanduono, R. F. Smith, D. G. Braun, J. R. Patterson, R. G. Kraus, T. S. Perry, A. Arsenlis, G. W. Collins, and J. H. Eggert, J. Appl. Phys. **117**, 245903 (2015).

[5] E. Moses, R. Boyd, B. Remington, C. Keane, and R. Al-Ayat, Phys. Plasmas 16, 041006 (2009).

[6] Bodner, Comments on Plasma Physics and Controlled Fusion, **16**, 351 (1995).

[7] A. L. Kritcher, R. Town, D. Bradley, D. Clark, S. Spears, O. Jones, S. Haan, P. T. Springer, J. Lindl, R. H. H. Scott, D. Callahan, M. J. Edwards, O. L. Landen, Phys. Plasmas, **21**, 042708 (2014).

[8] R. P. J. Town, D. K. Bradley, A. Kritcher, O. S. Jones, J. R. Rygg, R. Tommasini, M. Barrios, L. R. Benedetti, L. F. Berzak Hopkins, P. M. Celliers, *et al*, Phys. Plasmas, **21**, 056313 (2014).

[9] D. A. Callahan, O. A. Hurricane, J. E. Ralph, C. A. Thomas, K. L. Baker, L. R. Benedetti, L. F. Berzak Hopkins, D. T. Casey, T. Chapman, C. E. Czajka, E. L. Dewald, L. Divol, T. Doeppner, D. E. Hinkel, M. Hohenberger, L. C. Jarrott, S. F. Khan, A. L. Kritcher, *et. al*, Phys. Plasmas, **25**, 056305 (2018).

[10] J. Ralph, O. Landen, L. Divol, A. Pak, T. Ma, D. A. Callahan, A. Kritcher, T. Doeppner, D. E. Hinkel, C. Jarrott, J. D. Moody, B. B. Pollock, O. Hurricane, and M. J. Edwards, The Influence of hohlraum dynamics on implosion symmetry in indirect drive inertial confinement fusion, Phys. Plasmas, *submitted* (2018).

[11] O. A. Hurricane, D. A. Callahan, D. T. Casey, E. L. Dewald, T. R. Dittrich, T. Doeppner, S. Haan, D. E. Hinkel, L. F. Berzak Hopkins, O. Jones, A. L. Kritcher, S. Le Pape, T. Ma, A. G. MacPhee, J. L. Milovich, J. Moody, A. Pak, H.-S. Park, P. K. Patel, J. E. Ralph, H. F. Robey, J. S. Ross, J. D. Salmonson, B. K. Spears, P. T. Springer, et al., Nature Physics **12**, 800 (2016).

[12] T. R. Dittrich, O. A. Hurricane, D. A. Callahan, E. L. Dewald, T. Doeppner, D. E. Hinkel, L. F. Berzak Hopkins, S. LePape, T. Ma, J. L. Milovich, *et al.*, Phys Rev Letters, **112**, 055002 (2014).

[13] H.-S. Park, O. A. Hurricane, D. A. Callahan, D. T. Casey, E. L. Dewald, T. R. Dittrich, T. Doeppner, D. E. Hinkel, L. F. Berzak Hopkins, S. LePape *et al.*, Phys Rev Letters, **112**, 0550001, (2014).

[14] A. L. Kritcher, D. E. Hinkel, D. A. Callahan, O. A. Hurricane, D. Clark, D. T. Casey, E. L. Dewald, T. R. Dittrich, T. Doeppner, M. A. Barrios Garcia, S. Haan, *et al.*, Phys. Plasmas, **23**, 052709 (2016).

[15] D. S. Clark, C. R. Weber, J. L. Milovich, J. D. Salmonson, A. L. Kritcher, S. W. Haan, B. A. Hammel, D. E. Hinkel, O. A. Hurricane, O. S. Jones, M. M. Marinak, P. K. Patel, H. F. Robey, S. M. Sepke, and M. J. Edwards, Phys. Plasmas **23**, 056302 (2016).

[16] P. A. Michel, S. H. Glenzer, L. Divol, D. K. Bradley, D. Callahan, S. Dixit, S. Glenn, D. Hinkel, R. K. Kirkwood, J. L. Kline, W. L. Kruer, G. A. Kyrala, S. LePape, N.

B. Meezan, R. Town, K. Widmann, E. A. Williams, B. J. MacGowan, J. Lindl, and L. J. Suter, Phys. Plasmas, **17**, 056305 (2010).
[17] William L. Kruer, Scott C. Wilks, Bedros B. Afeyan, and Robert K. Kirkwood, Phys. of Plasmas **3**, 382 (1996).
[18] E. L. Dewald, J. L. Milovich, P. Michel, O. L. Landen, J. L. Kline, S. Glenn, O. Jones, D. H. Kalantar, A. Pak, H. F. Robey, G. A. Kyrala, *et al.*, Phys Rev Letters, **111**, 235001, (2013).
[19] G. A. Kyrala, J. L. Kline, S. Dixit, S. Glenzer, D. Kalantar, D. Bradley, N. Izumi, N. Meezan, O. Landen, D. Callahan, *et al.*, Phys. Plasmas, **18**, 056307 (2011).
[20] J. L. Milovich, E. L. Dewald, A. Pak, P. Michel, R. P. J. Town, D. K. Bradley, O. Landen, and M. J. Edwards, Phys. Plasmas, **23**, 032701 (2016).
[21] J. D. Moody, P. Michel, L. Divol, R. L. Berger, E. Bond, D. K. Bradley, D. A. Callahan, E. L. Dewald, S. Dixit, M. J. Edwards, S. Glenn, *et al.*, Nature Physics **8**, 344 (2012).
[22] L. F. Berzak Hopkins, N. B. Meezan, S. Le Pape, L. Divol, A. J. Mackinnon, D. D. Ho, M. Hohenberger, O. S. Jones, G. Kyrala, J. L. Milovich, A. Pak, *et al.*, Phys Rev Letters, **114**, 175001 (2015).
[23] D. Casey, C. Thomas, K. Baker, B. Spears, M. Hohenberger, S. Khan, R. Nora, C. Weber, A. Kritcher, T. Woods, *et. al*, Phys. Plasmas, *in preparation* (2018).
[24] A. Yi, A. Zylstra, S. MacLaren, J. Kline, Phys. Plasmas, *in preparation* (2018).
[25] L. Divol, A. Pak, L. F. Berzak Hopkins, S. Le Pape, N. B. Meezan, E. L. Dewald, D. D.-M. Ho, S. F. Khan, A. J. Mackinnon, J. S. Ross, D. P. Turnbull, *et al.*, Physics of Plasmas **24**, 056309 (2017).
[26] D. E. Hinkel, L. F. Berzak Hopkins, T. Ma, J. E. Ralph, F. Albert, L. R. Benedetti, P. M. Celliers, T. Doeppner, C. S. Goyon, N. Izumi, L. C. Jarrott, S. F. Khan, J. L. Kline, A. L. Kritcher, G. A. Kyrala, S. R. Nagel, A. E. Pak, P. Patel, M. D. Rosen, J. R. Rygg, M. B. Schneider, D. P. Turnbull, C. B. Yeamans, Phys Rev Letters, **117**, 225002 (2016).
[27] S. LePape, L. F. Berzak Hopkins, L. Divol, N. Meezan, D. Turnbull, A. J. Mackinnon, D. Ho, J. S. Ross, S. Khan, A. Pak, E. Dewald, *et al.*, Physics of Plasmas 23, 056311 (2016).
[28] O S Jones, C A Thomas, P A Amendt, G N Hall, N Izumi, M A Barrios Garcia, L F Berzak Hopkins, H Chen, E L Dewald, D E Hinkel, A L Kritcher, M M Marinak, N B Meezan, J L Milovich, J D Moody, A S Moore, M V Patel, J E Ralph, S P Regan, M D Rosen, M B Schneider, S M Sepke, DJ Strozzi and D P Turnbull, Journal of Physics: Conference Series **717** 012026 (2016).
[29] P. M. Celliers, D. K. Bradley, G. W. Collins, D. G. Hicks, T. R. Boehly, and W. J. Armstrong, Rev Sci. Instrum. 75, 4916 (2004).
[30] H. F. Robey, T. R. Boehly, P. M. Celliers, J. H. Eggert, D. Hicks, R. F. Smith, G. W. Collins, M. W. Bowers, K. G. Krauter, P. S. Datte, *et al.*, Phys. Plasmas. 19, 042706 (2012).
[31] J. R. Rygg, O. S. Jones, J. E. Field, M. A. Barrios, L. R. Benedetti, G. W. Collins, D. C. Eder, M. J. Edwards, J. L. Kline, J. J. Kroll, O. L. Landen, T. Ma, A. Pak, J. L. Peterson, K. Raman, R. P. J. Town, and D. K. Bradley, Phys Rev Letters **112**, 195001 (2014).
[32] J. Ralph, Experimental results for N170706 and N161103.
[33] M. M. Marinak, G. D. Kerbel, N. A. Gentile, O. Jones, D. Munro, S. Pollaine, T. R. Dittrich, and S. W. Haan, Phys. Plasmas **8**, 2275 (2001).
[34] M.D.Rosen, H.A. Scott, D.E. Hinkel, E.A. Williams, D.A. Callahan, R.P.J. Town, L. Divol, P.A. Michel, W.L. Kruer, L.J. Suter, R.A. London, J.A. Harte, G.B. Zimmerman, High Energy Density Phys. **7**, 180 (2011).
[35] C. A. Iglesias and F. J. Rogers, Astrophys. J. 464, 943 (1996).
[36] J. D. Moody, D. J. Strozzi, L. Divol, P. Michel, H. F. Robey, S. LePape, J. Ralph, J. S. Ross, S. H. Glenzer, R. K. Kirkwood, O. L. Landen, B. J. MacGowan, A. Nikroo, and E. A. Williams, Phys Rev Letters, **111**, 025001 (2013).
[37] O.S. Jones, C. J. Cerjan, M. M. Marinak, J. L. Milovich, H. F. Robey, P. T. Springer, L. R. Benedetti, D. L. Bleuel, E. J. Bond, D. K. Bradley, *et al.*, Phys. Plasmas. **19**, 056315 (2012).
[38] A. L. Kritcher, D. Clark, S. Haan, S. A. Yi, A. B. Zylstra, D. A. Callahan, D. E. Hinkel, L. F. Berzak Hopkins, O. A. Hurricane, O. L. Landen, *et al.*, Phys. Plasmas, **25**, 056309 (2018).
[39] S. F. Khan, J. J. Lee, N. Izumi, B. Hatch, G. K. Larsen, A. G. MacPhee, J. R. Kimbrough, J. P. Holder, M. J. Haugh, Y. P. Opachich, P. M. Bell, and D. K. Bradley, Proc. SPIE 8505, **05** (2012).
[40] D. J. Strozzi, D. S. Bailey, P. Michel, L. Divol, S. M. Sepke, G. D. Kerbel, C. A. Thomas, J. E. Ralph, J. D. Moody, and M. B. Schneider, Phys Rev Letters, **118**, 025002 (2017).
[41] I. V. Igumenshchev, W. Seka, D. H. Edgell, D. T. Michel, D. H. Froula, V. N. Goncharov, R. S. Craxton, L. Divol, R. Epstein, R. Follett, *et al*, Phys. Plasmas **19**, 056314 (2012).
[42] T. Chapman, Calculated SBS in low gas filled hohlraums.
[43] J. D. Moody, D. J. Strozzi, L. Divol, P. Michel, H. F. Robey, S. LePape, J. Ralph, J. S. Ross, S. H. Glenzer, R. K. Kirkwood,1 O. L. Landen, *et al.*, Phys Rev Letters, **111**, 025001(2013).
[44] T. Dppner B. Bachmann, F. Albert, P. Bell, S. Burns, J. Celeste, R. Chow, L. Divol, E.L. Dewald, M. Hohenberger, C.M. Huntington, *et al*, JINST,**11** (2016).
[45] John A. Oertel, Cris Barnes, Tom Archuleta, Larry Casper, Valerie Fatherley, Todd Heinrichs, Robert King, Doug Landers, Frank Lopez, Phillip Sanchez, George Sandoval, Lou Schrank, Peter Walsh, *et al.*, Rev. Sci. Instrum. **77**, 10E308 (2006).
[46] A. K. Davis, D. Cao, D. T. Michel, M. Hohenberger, D. H. Edgell, R. Epstein, V. N. Goncharov, S. X. Hu, I. V. Igumenshchev, J. A. Marozas, *et al*, Phys. Plasmas **23**, 056306 (2016).
[47] P. Michel, W. Rozmus, E. A. Williams, L. Divol, R. L. Berger, S. H. Glenzer, and D. A. Callahan, Physics of Plasmas **20**, 056308 (2013).
[48] G. N. Hall, O. S. Jones, D. J. Strozzi, J. D. Moody, D. Turnbulla), J. Ralph, P. A. Michel, M. Hohenberger, A. S. Moore, O. L. Landen, L. Divol, D. K. Bradley, D. E. Hinkel, A. J. Mackinnon, R. P. J. Town, N. B. Meezan, L. Berzak Hopkins, and N. Izumi, Phys. of Plasmas **24**, 052706 (2017).
[49] O.A. Hurricane, D.A. Callahan, M. J. Edwards, P. Patel, K. Baker, D.T. Casey, L. Divol, T. Do?ppner, D.E. Hinkel, M. Hohenberger, L.F. Berzak Hopkins, A. Kritcher, *et al*, in progress (2018).

	1ω wavelength(Å)		
Shot number	23^{o}cone	30^{o}cone	44^o&50^o cone
N161006-002	10530.5	10530.5	10528.5
N161103-001	10529.8	10529.8	10524.3
N170706-001	10530.5	10529.8	10524.3

TABLE I. Operation wavelengths for the inner (23^o&30^o) laser beam cones and outer (44^o&50^o) laser beam cones.

APPENDIX